Sulfonated PBI Gel Membranes for Redox Flow Batteries

Lihui Wang,[1,=] Andrew T. Pingitore,[1,=,*] Wei Xie,[2] Zhiwei Yang,[2,] Michael L. Perry,[2] and Brian C. Benicewicz[1,**,z]**

[1]*Department of Chemistry and Biochemistry, University of South Carolina, Columbia, South Carolina, USA*
[2]*United Technologies Research Center, East Hartford, Connecticut, USA*

Sulfonated polybenzimidazole (s-PBI) gel membranes were prepared and shown to have a high stability in concentrated sulfuric acid and strongly oxidizing vanadium (V) solutions. These membranes were considered candidates for use in vanadium redox flow batteries, and compared to the commonly used "conventionally imbibed" *meta*-polybenzimidazole (m-PBI) membranes cast from N,N'-dimethylacetamide (DMAc) solutions. The s-PBI membranes exhibited high conductivities (up to ~240 mS cm^{-1}) and low performance degradation during in-cell testing.

 [DOI: 10.1149/2.0471908jes]

Manuscript submitted December 21, 2018; revised manuscript received April 10, 2019. Published April 29, 2019.

Increasing demands on the energy sector have created a new need for large-scale energy storage devices with additional implications in grid management and back-up power, coincidentally with the seamless integration of new renewable energy devices. Redox flow batteries have the potential to both efficiently store large amounts of energy as well as meet cost expectations.[1,2] In a vanadium redox flow battery (VRB) a major portion of the cost is attributed to the vanadium electrolyte. This cost can be off-set with high power density cells, which enables smaller and less expensive cell stacks. Currently, in commercial VRBs, PFSA membranes are used in the stack component, which has limited the forward progress due to their low selectivity and high cost.[1–4] To reduce costs of VRBs and increase overall performance, there has been a surge in membrane development activities tailored to the specific needs of VRBs. Up to the present time, various low cost polymer-electrolyte membranes have been studied such as sulfonated poly(sulfone),[5] sulfonated poly(ether ether ketone) (SPEEK) membranes,[6,7] quaternized cardo-poly (ether ketone) based membranes[8] and polybenzimidazole.[9–11]

Phosphoric acid (PA) doped polybenzimidazole (PBI) membranes are most notably known for their performance in high temperature polymer electrolyte membranes (HT-PEMs). However, PBI membranes have been shown to be a favorable candidate for multiple new devices, such as electrochemical hydrogen separation, SO_2 depolarized electrolyzers, and redox flow batteries. To date, research on PBI membranes for flow batteries has focused around *meta*-polybenzimidazole (m-PBI) and its derivatives. For these polymers, membranes were prepared by solution casting in N,N'-dimethylacetamide (DMAc) to form a dense film and later imbibing the formed film in the desired electrolyte, representing a process called the "conventional imbibing process."[12] Membranes prepared by this method typically have pore sizes that range from 0.5 nm to 2.0 nm,[9] which is much smaller than the pore sizes found in PFSA (e.g., Nafion) type membranes (2-4 nm).[13] This decrease in interstitial space allows for the dramatically decreased permeability of vanadium ions compared to PFSA membranes, but also accounts for its extremely low conductivities when imbibed in common VRB electrolyte solutions (<20 mS·cm^{-1}).[9,10,14–16] The focal point of these recent works is to enhance the proton conductivity while maintaining the inherently low permeability of m-PBI dense films. These techniques include: pre-swelling the PBI films in concentrated phosphoric acid before doping with sulfuric acid,[15] using the vapor induced phase inversion method,[13] creating a cage-like porous carbon with super high activity and entrapping the redox couples,[17] introducing partial pendant hydrophilic trimethylamine (TMA) groups on the pore walls of porous membranes,[18] non-solvent induced phase separation to create a spongy porous structure,[14] and the grafting of various substituents to the PBI polymer backbone.[16,19] To the best of our knowledge, no research has been conducted on the use of PBI gel membranes, formed from the PPA Process,[20] as alternative membranes for redox flow batteries.

The conventional imbibing process of PBI membranes is a time consuming, environmentally unfriendly technique that adds cost to the membrane fabrication process. However, Xiao et al. developed the novel PPA process to prepare PBI gel membranes which consists of a direct casting of the polymerization solution[20] comprising the PBI polymer in polyphosphoric acid (PPA). Subsequent exposure of the cast solution to atmospheric moisture or controlled humidity conditions at room temperature hydrolyzes the PPA solvent, a good solvent for many PBIs, to phosphoric acid (PA), which is a poor solvent for many PBIs. This process induces a solution to gel transition forming a PBI gel membrane inherently imbibed in phosphoric acid.[20] Although these membranes are "pre-imbibed" in phosphoric acid, it has been shown that these membranes are capable of undergoing acid exchange of the imbibed electrolyte. Garrick et al. exchanged the phosphoric acid in sulfonated *para*-polybenzimidazole (s-PBI) membranes with 50 wt% sulfuric acid solutions for testing in a SO_2 depolarized electrolyzer used to generate hydrogen. The membrane exhibited high stability in concentrated sulfuric acid, even at 120°C. Furthermore, the membrane resistance in the SO_2 depolarized electrolyzer was found to be almost negligible in comparison to the anodic overpotential, and this was attributed to the high ionic conductivity of s-PBI.[21,22] Due to the exceptional stability of this PBI derivative and its high conductivity, we envisioned s-PBI polymer gel membranes to be a possible alternative membrane for VRB cells with high performance capabilities.

Experimental

Materials.—3,3',4,4'-Tetraaminobiphenyl (TAB, polymer grade, ~97.5%) was donated by BASF Fuel Cell, Inc. and used as received. Monosodium 2-sulfoterephthalate (>98.00% purity) was purchased from TCI and used as received. Polyphosphoric acid (115%) was supplied from FMC Corporation and used as received. α,α'-Dichloro-p-xylene (>98.0% purity) was purchased from TCI and used as received.

Polymer synthesis and membrane fabrication.—A typical polymerization consisted of 10.71 g tetraaminobiphenyl (TAB, 50 mmol), and 13.44 g monosodium 2-sulfoterephthalate (s-TPA, 50 mmol) added to 580 g polyphosphoric acid, mixed with an overhead stirrer and purged with dry nitrogen. The contents were heated in a high temperature silicone oil bath, and the temperature was controlled by a programmable temperature controller with ramp and soak features. The reaction temperature was increased stepwise to 120°C, 150°C, 170°C and 195°C. In a typical polymerization, the final reaction temperature was approximately 195°C and held for 12 hours. Once the reaction was completed, determined by visual inspection of viscosity, the polymer solution was cast onto clear glass plates using a doctor

[=]These authors contributed equally to this work.
[*]Electrochemical Society Student Member.
[**]Electrochemical Society Member.
[z]E-mail: benice@sc.edu

blade with a controlled gate thickness of 15 mils. The cast solution was hydrolyzed into membranes in a humidity chamber regulated to 55% R.H. at 25°C.

Acid exchange.—As-cast membranes were placed in DI water baths, and the pH of the water was monitored using pH strips. Water baths were replaced every 8 hours until a pH of 7 was recorded. At this point the membrane was either placed into a 2.6 M sulfuric acid bath for 24 hours to ensure equilibrium of acid doping, or the membrane was further modified by a crosslinking reaction.

Post-membrane formation crosslinking.—After PA removal the PBI gel membranes were allowed to soak in a bath of 0.0523 M solution of α,α'-dichloro-p-xylene in methanol. The bath was covered, heated to 30°C, and agitated with a magnetic stir bar. Crosslinking reactions were typically allowed to proceed for 6 hours. The membrane was then washed with DI water and methanol cyclically, at least three times. The membrane was then transferred to a 2.6 M sulfuric acid (SA) bath for 24 hours for acid doping.

Membrane composition.—The composition of sulfuric acid-doped PBI membranes was determined by measuring the relative amounts of polymer solids, water, and acid in the membranes. The sulfuric acid (SA) content of a membrane was determined by titrating a membrane sample. After the s-PBI membrane sample was removed from 2.6 M SA, the membrane was wiped to remove excess liquid and weighed. Then the sample was put in 20 ml DI water and stirred at 35°C overnight to leach the acid from the membrane. A standardized sodium hydroxide solution (0.10 M) was used to titrate the sample using a Metrohm 888 DMS Titrando autotitrator. Once titrated, the sample was thoroughly washed with DI water and dried at reduced pressures at 120°C overnight. The dried sample was then weighed to determine the polymer solids content of the membrane.

Using Equations 1 and 2, the polymer weight percentage and sulfuric acid weight percentage can be determined, respectively;

$$Polymer\ w/w\ \% = \frac{W_{dry}}{W_{sample}} \cdot 100 \quad [1]$$

$$Acid\ w/w\ \% = \frac{M_{acid} \cdot V_{NaOH} \cdot c_{NaOH}}{2 \cdot W_{sample}} \quad [2]$$

where W_{sample} is the weight of the sample before titration, W_{dry} is the weight of final dried sample after titration, M_{acid} is the molecular weight of sulfuric acid, and V_{NaOH} and c_{NaOH} are the volume and concentration of the sodium hydroxide solution required to neutralize the sulfuric acid to the first equivalence point. It is important to note that even though the second proton of sulfuric acid is much less acidic than the first, it is still a strong enough acid to cause both protons to be titrated simultaneously, $pK_{a1} = -3$ and $pK_{a2} = 2$.

Ionic conductivity.—The membranes were imbibed with sulfuric acid and V^{4+} ions by immersion in both 2.6 M sulfuric acid and a VRB electrolyte solution, 1.5 M $VOSO_4$ in 2.6 M sulfuric acid, which is the fully-discharged VRB posolyte solution. In-plane conductivity of the membrane was measured by a four-probe electrochemical impedance spectroscopy (EIS) method using a FuelCon (TrueData EIS PCM) electrochemical workstation over the frequency range from 1 Hz to 50 kHz. A membrane sample with a typical geometry of 1.0 cm × 4.0 cm was fixed into the measuring 4-electrode head of the instrument. The ionic conductivity of the membrane was calculated using the following equation:

$$\sigma = \frac{d}{l \cdot w \cdot R_m} \quad [3]$$

where d is the distance between the two inner probes, l is the thickness of the membrane, w is the width of the membrane, and R_m is the ohmic resistance determined by the model fitting. Conductivities were measured at room temperature (23°C), which is within the normal operating conditions of VRB systems (typically 20 to 50°C).

Tensile testing.—Mechanical properties of s-PBI, s-PBI-x and conventional imbibed m-PBI were evaluated in tension using an Instron 5543A mechanical tester. The membrane samples were taken from the DI water bath and cut into Type 5 dogbone shaped specimens. The membranes were stretched at r.t. at 20mm min^{-1} until failure. The stress-strain curves were used to record the stress and elongation at the break.

Vanadium permeability.—The crossover of vanadium(IV) ($VOSO_4$) was measured utilizing a PermeGear "side-by-side" direct permeation cell. The cell has two chambers with a 45 mL volume separated by the membrane under test. The temperature of the chambers was regulated at 25°C with a recirculating water bath. A typical test experiment contained 1.5 M $VOSO_4$ in 2.6 M sulfuric acid in the donor chamber and 1.5 M $MgSO_4$ in 2.6 M sulfuric acid in the receptor chamber. The concentration of vanadium(IV) in the receptor chamber was measured using the strong absorption at 248 nm with a Shimadzu UV-2450 UV/Vis spectrometer at various time intervals. The VO^{2+} permeability can be calculated using Fick's diffusion law, Equation 4,

$$P_s t = ln\left[1 - 2\frac{c_r(t)}{c_r(0)}\right]\left[-\frac{Vd}{A}\right] \quad [4]$$

where: $c_r(t)$ is the receptor $VOSO_4$ concentration at time t, $c_r(0)$ is the donor initial $VOSO_4$ concentration, V is the donor and receptor solution volume, d is the membrane thickness, A is the active area of the membrane, and P_s is the salt permeability.[4]

Membrane stability in oxidative V(V) solution.—Membranes were soaked in a solution of 1.5 M V^{5+} in 2.6 M sulfuric acid. The solution was periodically titrated using a Hiranuma Auto Titrator COM-1700 against a control solution that did not contain a polymer membrane to measure the concentration of V^{5+} and V^{4+} ions.

Flow battery cell and durability test.—The VRB test cell consisted of 24 cm^2 active area and utilized interdigitated flow fields for liquid electrolyte solutions machined into carbon plates (Tokai G347B), designed and assembled by United Technologies Research Center (UTRC). The membranes were sandwiched between identical carbon paper electrodes provided by UTRC that were heat treated to 400°C for 30 hours in air, and gasketed with polytetrafluoroethylene (PTFE) films. The charge/discharge cycling performance was measured at constant current densities ranging from 0.072 A/cm^2 to 0.484 A/cm^2 using a multi-channel potentiostat (Model BT2000, Arbin Instrument Inc., College Station, TX).

For each current density (identical and constant during charge and discharge), the cell was equipped with two reservoirs starting with 100 mL of new electrolyte per side, which consisted of 1.60 M of vanadium species having 3.55 average oxidation state and 4.2 M total sulfur content (Riverside Specialty Chemicals Inc. New York, NY). The electrolytes were circulated through the cell at a constant flow rate of 120 mL/min by two acid-resistant diaphragm pumps (KNF Neubarger). A stream of humidified nitrogen was purged through the head space of the reservoirs to prevent air intrusion during testing. The cell and electrolyte solution temperature were not controlled and were approximately 20°C. The cell was initially charged by 2A constant current to create the posolyte in the positive side and the negolyte in the negative side, as has been described elsewhere.[23] Then the cell was continuously charge/discharge cycled for 23 cycles between the cell's voltages described in Table I, which led to approximately 80% SOC at the end of the charge and approximately 20% SOC at the end of the discharge. The average round-trip cycling efficiencies of cycles #4 to #14 are presented (Figure S1) and discussed in the Results and Discussion.

The in situ chemical stability test was conducted by examining the FTIR and inherent viscosity (I.V.) of membranes. The membranes after cell testing were washed with DI water several times until all the

Table I. The cell voltage window for charge/discharge cycling tests.

Charge/discharge density	Cell voltage at the end of charge	Cell voltage at the end of discharge
0.072 A/cm^2	1.525 V	1.150 V
0.242 A/cm^2	1.610 V	1.100V
0.483 A/cm^2	1.725 V	1.000V

acid and vanadium ions were removed. The samples were then dried at 120°C for FT-IR and I.V. measurements. Attenuated total reflectance (ATR) infrared spectra were recorded using a Perkin-Elmer Spectrum 100-FTIR with diamond/ZnSe triple reflection crystal. After dissolution of samples in 96% sulfuric acid at 0.2g dL^{-1} concentrations, IVs were measured using an Ubbelohde viscometer equilibrated in a water bath set at 30.0°C. Inherent viscosity was calculated by Equation 5,

$$\ln\left[(t)\,(t_0)^{-1}\right]c^{-1} = Inherent\ Viscosity\ \left(dL\,g^{-1}\right) \qquad [5]$$

Results and Discussion

The area power density of a flow battery is highly dependent on the ionic conductivity of the membrane. m-PBI membranes prepared from the conventional imbibing process have relatively low conductivities, which prevents operation at high current densities and high efficiencies. Herein, we investigate the use of a highly conductive membrane, s-PBI, for their use in VRB cells, Scheme 1.

The ex-situ membrane properties for s-PBI gel membranes (both uncrosslinked and crosslinked) and m-PBI membranes formed from the conventional imbibing process are shown in Table II. The room

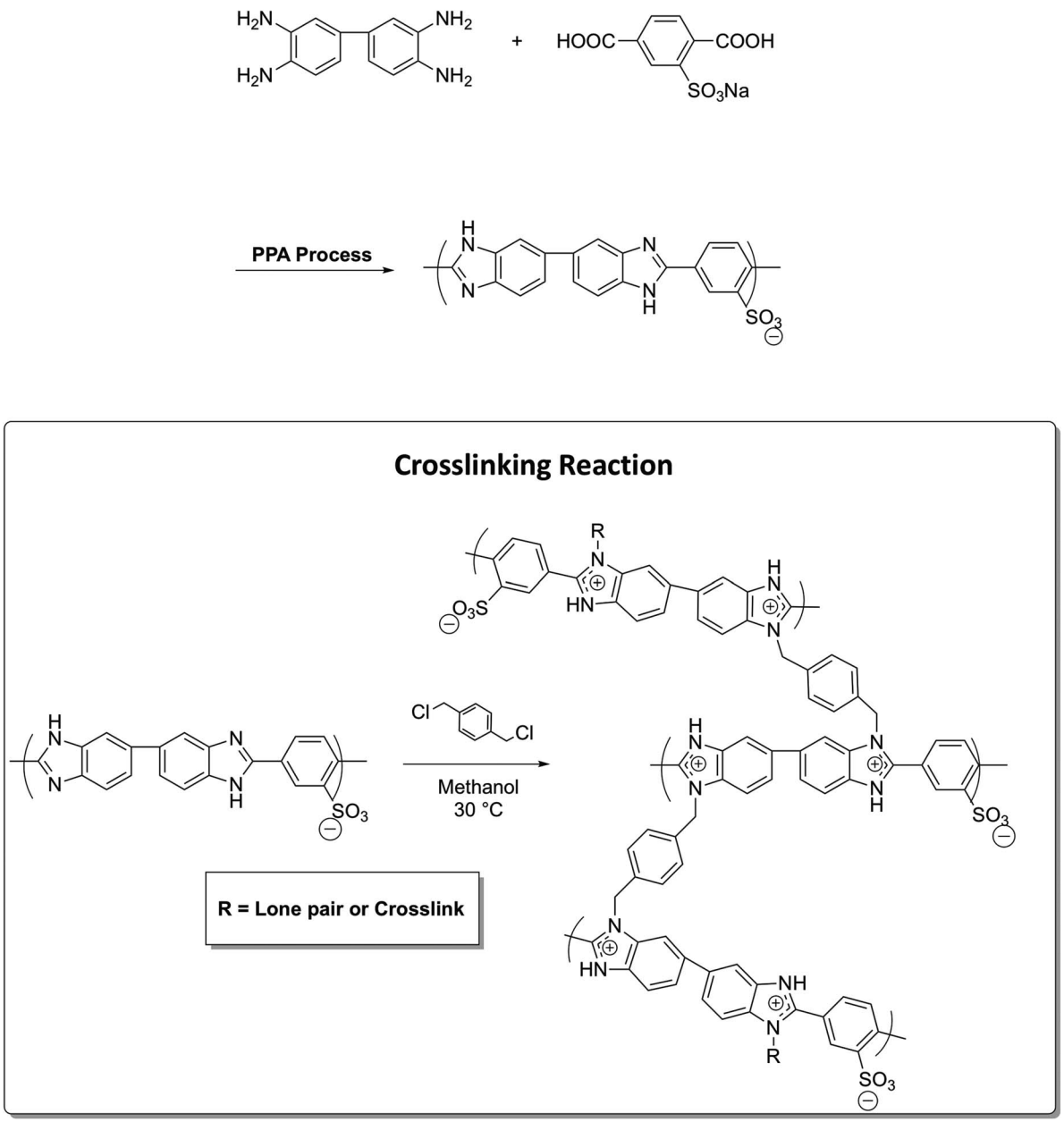

Scheme 1. Polymerization of s-PBI in PPA and membrane crosslinking modification reaction.

Table II. Ex-situ properties of s-PBI membranes, conventional m-PBI films and Nafion 212.

Membrane	VO^{2+} Permeability ($cm^2 \cdot s^{-1}$)	Wet thickness (μm)	Conductivity ($mS \cdot cm^{-1}$)[a]	Conductivity ($mS \cdot cm^{-1}$)[b]	Polymer content (wt%)	SA content (wt%)	Water Content (wt%)
s-PBI	5.74×10^{-7}	220.2	592.7	242.1	18.8	23.1	58.1
s-PBI-x	5.23×10^{-7}	269.3	537.3	240.2	30.6	35.6	33.8
m-PBI (conventionally imbibed)	2.53×10^{-11}	40.1	13.1	12.2	65.6	26.0	8.4
Nafion 212	6.40×10^{-9}	51.5	44.5	23.1	N/A	N/A	5.0*

[a]Conductivity at r.t. after soaking in 2.6 M sulfuric acid.
[b]Conductivity at r.t. after soaking in V(IV)/H^+ solution (1.5 M $VOSO_4$ + 2.6 M sulfuric acid) for 3 days.
*The data is from Nafion information sheet for the membrane, as-received.

temperature conductivity of the membranes was evaluated in both 2.6 M sulfuric acid and a V(IV)/H^+ solution found in typical operating cell conditions. s-PBI gel membranes exhibit much higher conductivities as compared to the m-PBI membranes in both sulfuric acid and the VRB-electrolyte solution. The room temperature conductivities of the s-PBI and crosslinked s-PBI membranes were in the range of 537–593 $mS \cdot cm^{-1}$ compared to 13.1 $mS \cdot cm^{-1}$ for conventionally imbibed *m*-PBI in sulfuric acid and 240–242 $mS \cdot cm^{-1}$ compared to 12.2 $mS \cdot cm^{-1}$ in the VRB electrolyte, respectively.

The slight difference in conductivity in sulfuric acid between the two s-PBI membranes is likely a result of cross-linking. s-PBI-x in Table II is a s-PBI film that underwent a cross-linking modification post-hydrolysis of the membrane. The crosslinker forms bonds with the imidazole nitrogen and may slightly inhibit proton pathway through the hydrogen bond networks. When comparing imbibed solutions, the differences in conductivity of the gel membranes in VRB-electrolyte solutions is largely eliminated. The general differences in conductivities when comparing pure sulfuric acid and VRB-electrolyte imbibed membranes is thought to occur from two factors. The first is that vanadium ions may interact with the membrane by attractive forces with the negatively charged sulfonate group (pKa ~ -2), impeding the flow of other cations. The decrease in conductivity in the PBI gel membranes is most likely attributed to the lower intrinsic conductivity of the VRB posolyte solution in the discharged state, which is approximately 3.5X lower than 2.6M sulfuric acid at room temperature, where 1.5M V^{4+} and 4M sulfate is 229 mS/cm and 2.6M sulfuric acid is 800 mS/cm.[24] The second factor that contributes to the decrease in ionic conductivity of the VRB electrolyte solution is the increase in viscosity of the VRB electrolyte relative to an acid-only solution.[25] PBI gel membranes have a considerably open morphology that enhances ionic conductivity by allowing not only cation transport via the Grotthuss mechanism but also mobility of the electrolyte in the membrane, thus ion transport through the membrane will also be affected by the increase in viscosity due to the incorporation of vanadium ions.

The electrolyte mobility in the PBI gel membrane is a plausible rationalization to explain the higher vanadium permeability compared to the conventionally imbibed membrane. This result is also not unexpected when considering the polymer solids of the membrane. From the data in Table II it is evident s-PBI membranes have a relatively small amount of polymer relative to the amount of electrolyte in the membrane compared to m-PBI. With the expectation of PBI gel membranes possessing higher crossover of vanadium ions, we devised a mitigation route to chemically crosslink the PBI chains to fill interstitial space and limit chain mobility. Although the permeability of the s-PBI-x may still be too high for practical applications this slight modification does lower the permeability when compared to the non-crosslinked membrane and without having a negative effect on conductivity. Since this technique can be applied to many PBI derivatives, it could be used to further adjust the properties of PBI membranes as needed. At this time, we have not found a facile way to determine the cross-link density of the gel membrane, as typical gravimetric and rheological techniques carry large amounts of error with as-cast imbibed gel membranes.[26–28] However, to confirm crosslinking occurred, a 50 mg sample of neutralized dried membrane was heated in 800 mL N,N'-dimethylacetamide at reflux for 48 hours. Under these conditions no membrane deterioration or solution color change was observed for the crosslinked sample, but dissolution was observed for the non-crosslinked polymer film.[29]

The polymer composition was then analyzed by infrared spectroscopy (IR) (Figure 1). Initially, triple pass attenuated total reflectance IR spectroscopy was used to confirm the presence of the sulfonic acid moiety in the polymer structure for PPA processed films. Three regions of signals showing the presence of the sulfonic acid groups were observed and are consistent with the literature.[30] The peak at 800 cm^{-1} corresponds to the symmetric S-O bond, meanwhile the peaks at 1022 and 1070 cm^{-1} arise from the S = O symmetric double bonds. There are strong bands at 1164 and 1225 cm^{-1} corresponding to the asymmetric stretching of S = O. Typical absorption bands from the benzimidazole ring appear in the range 1650-1500 cm^{-1} and are characteristic of the C=C/C=N stretching vibrations in the imidazole. Additionally, the absence of a strong band in the 1700-1650 cm^{-1} region is indicative of complete ring closure of the imidazole ring.

Table III shows the average stress and strain at break results for water imbibed s-PBI, s-PBI-x, conventional m-PBI and Nafion 212 membranes while Figure 2 shows representative stress-strain curves for water imbibed s-PBI, s-PBI-x and conventional m-PBI membranes. The conventional m-PBI film has much higher stress at break (~119 MPa), and a strain at break of 21% suggesting it is a hard and strong film. In contrast, s-PBI gel membranes prepared via PPA process showed different material properties. The average stress at break values were 2.8 and 7.8 MPa, while the strain at break values were 35.4% and 66.0% for s-PBI and s-PBI-x respectively. Thus these materials are softer and more elastic material and clearly reflect the higher water content of the sulfonated PPA processed materials. It is interesting to note that the open structure of the membrane is retained, even through multiple acid and water exchange steps. The s-PBI-x membranes showed higher mechanical properties than the s-PBI membranes and illustrates that crosslinking can be used to increase the mechanical properties in PBI gel-type membranes.

There are four common oxidation states for vanadium, all of which are present in the VRB electrolyte during normal operation. Of these, VO_2^+ [V(V)] bears the highest oxidation state (+5). The facile reduction of this compound makes it a good oxidizing agent. During VRB operation, VO_2^+ is present in increasing concentrations as the battery is being charged. Due to its oxidative nature and the potential for prolonged interactions with the membrane separator, it is imperative to study the stability of the membrane under such oxidative conditions. The oxidative stability of the s-PBI base polymer was monitored by soaking a membrane in 2.6 M sulfuric acid with approximately 1.5 M of V(V). Over the course of 1 year soaking in this fully-charged VRB posolyte solution, various titration measurements were conducted to determine the concentration of V(V) remaining and the presence of V(IV) which would be produced consequently from membrane oxidation (vanadium reduction). Table IV shows that the concentration of V(V) is consistent with the control bath (no membrane) and the lack of V(IV) present suggests that s-PBI polymers are stable under

Figure 1. ATR-FTIR spectra of a) s-PBI membrane before cell testing; b) s-PBI membrane after cell testing; c) s-PBI-x membrane before cell testing; b) s-PBI-x membrane after cell testing. All membranes were examined after treatment overnight at 120°C.

these harsh conditions. This stability is not common for fully organic polymer membranes.[31]

Membranes were tested in flow battery cells designed and assembled by United Technologies Research Center with specialized flow fields for liquid electrolytes. Figure 3A shows polarization curves from 0–1.1 A/cm^2. The inability of conventionally imbibed m-PBI membranes to operate at high current densities is clearly apparent. This is attributed to the low ionic conductivity of the densely packed morphology. Both the s-PBI and its cross-linked form have relatively high acid doping levels and high ionic conductivity, which allows them to perform at substantially higher currents densities. This is also reflected in the relatively high voltage efficiencies, Figure 3B, where the voltage ratio of discharge to charge at 483.3 mA/cm^2 is similar to that of conventionally imbibed m-PBI at a current density that is 6.7X lower (71.7 mA/cm^2). Since conventionally imbibed m-PBI performed poorly under these test conditions, cycling efficiencies could not be assessed beyond 200 mA/cm^2.

Furthermore, there is only a slight difference in performance and voltage efficiency between the s-PBI and s-PBI-x. This can be explained by the slightly higher conductivity of s-PBI compared to s-PBI-x. However, the coulombic efficiency, the ratio of electrons discharged to charged, is lower and particularly noticeable at low current

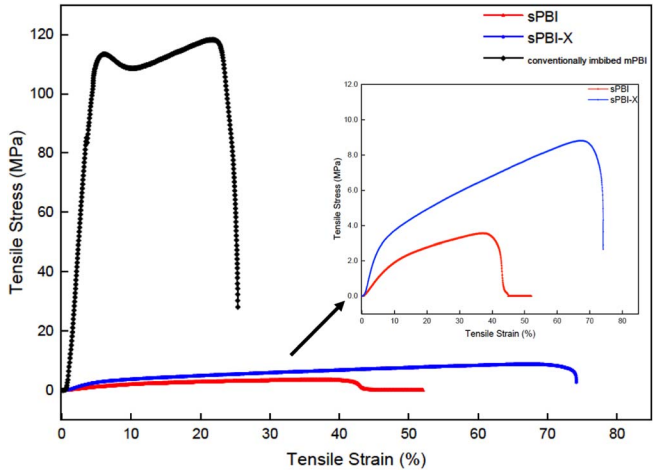

Figure 2. Stress-strain curves for water imbibed s-PBI (80.4 ± 0.7% H_2O), s-PBI-x (76.8 ± 0.3% H_2O) and conventional m-PBI (16.3 ± 2.9% H_2O) membranes.

Table III. Tensile test results of s-PBI membranes, conventional m-PBI films and Nafion 212.

Membrane	s-PBI	s-PBI-x	m-PBI (conventionally imbibed)	Nafion 212
Stress at break (MPa)	2.8 ± 0.4	7.8 ± 1.2	119.0 ± 0.6	32[a]
Strain at break (%)	35.4 ± 2.8	66.0 ± 14.2	21.0 ± 4.5	3.5[a]

Note: The data for the pristine samples give error bars derived from the calculated standard error for n = 3 measurements.
[a]The data is from Nafion information sheet.

Table IV. Oxidative stability of sulfonated PBI gel membranes in V^{5+} solutions.

	Titration Date (t = 267 days)		Titration Date (t = 401 days)	
Membrane	V^{4+}(mol/L)	V^{5+}(mol/L)	V^{4+}(mol/L)	V^{5+}(mol/L)
V^{5+} Control	Non-detectable	1.570	Non-detectable	1.583
s-PBI	Non-detectable	1.551	Non-detectable	1.576

densities, attributable to the crossover of reaction species (Figure 3C). It is important to note that this contribution to inefficiency is reduced at high current densities where the increased reaction speed can outpace parasitic losses from crossover. The overall energy efficiency, a product of coulombic and voltage efficiencies, is a useful metric to determine the amount of energy lost during charge/discharge cycling. The results shown in Figure 3D indicate a promising potential use of PBI gel membranes formed from the PPA process. Even at low current densities, where the coulombic inefficiency is most pronounced, both s-PBI and s-PBI-x have similar or even greater energy efficiency compared to conventionally imbibed m-PBI because the high voltage efficiency compensates for those losses. At high current densities, the unmodified s-PBI membrane displays a slightly higher energy efficiency than the crosslinked s-PBI. A major advantage of the VRB system is that the energy capacity of the battery can be fully recovered by simply redistributing the V ions. For example, a simple recovery method is to fully mix the posolyte and negolyte and then redistribute this fully-mixed solution between the two reservoirs at certain intervals.[32] Alternatively, one can redistribute small amounts of V between the posolyte and negolyte at more frequent intervals, and this distribution of V can also be based on the average oxidation state of the V to maximize the energy capacity as the oxidation state of the electrolyte varies with extended operations due to side reactions.[33] Nonetheless, high V crossover is not desirable in a VRB membrane, and crosslinking proves to be a viable approach for reducing this characteristic.

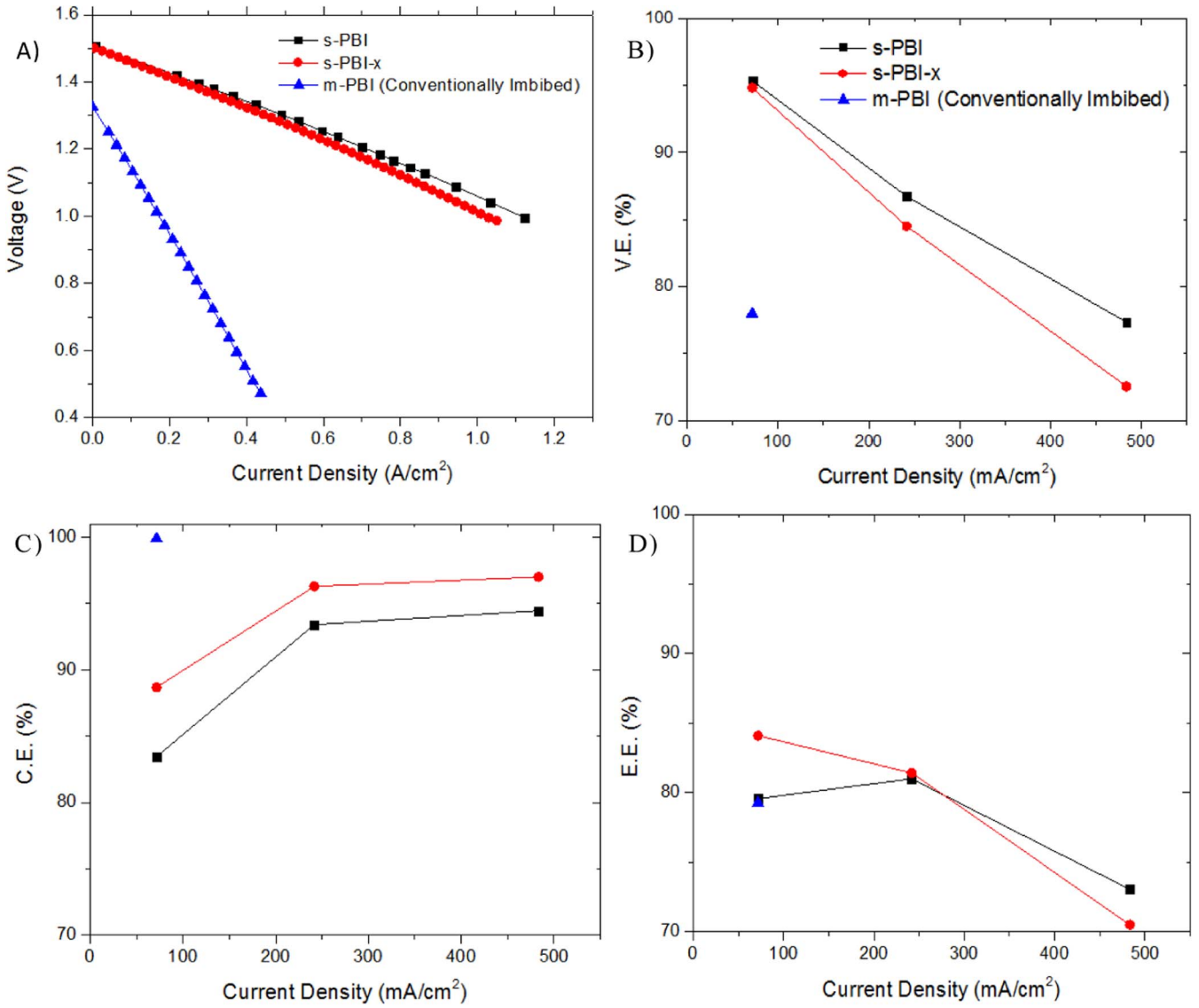

Figure 3. A) Polarization curves with 80% state-of-charge electrolyte, and cycling efficiencies: B) voltage efficiencies, C) coulombic efficiencies, and D) energy efficiencies of VRB cells that were otherwise identical but utilized with three different membranes: s-PBI, s-PBI-x, and m-PBI (conventionally imbibed).

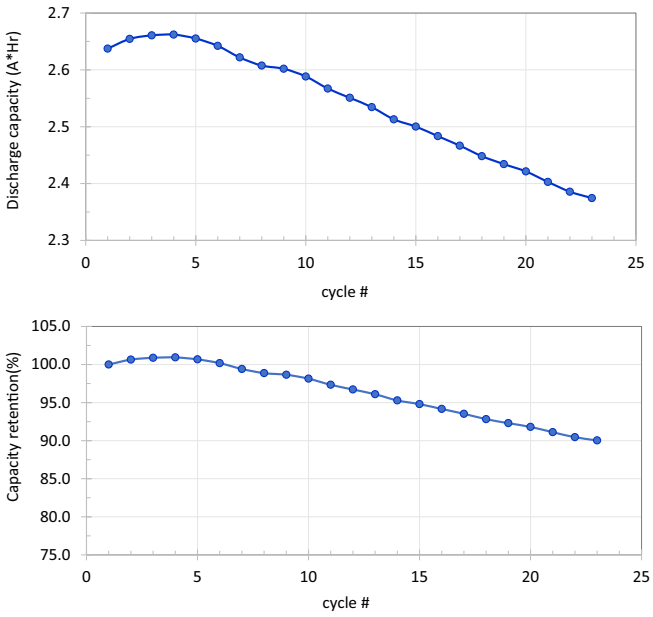

Figure 4. Discharge capacities and and capacity retention of VRB with s-PBI-x membrane in 23 cycles.

The stability of membranes after long term cycling is one of the most challenging problems in large-scale VRB applications. The durability of s-PBI-x membranes in VRB cell testing and the capacity decay was measured by operating the VRB for 23 cycles under a high current density of 242 mA cm^{-2}. The discharge capacity curve and capacity retention after 23 cycles for VRB single cell with s-PBI-x membrane are illustrated in Figure 4. As shown, the discharge capacity maintained 90.02% after 23 cycles compared with the initial cycle. The capacity fade may result from the high crossover contamination of vanadium ions which corresponds to a higher vanadium permeability for PBI gel membranes. The rough current density testing condition in this work could also be a factor of capacity decay.

The chemical stability of s-PBI membranes was analyzed by comparing the FT-IR spectra before and after VRB cell testing. As shown in Figure 1, these peaks were unchanged after cell testing for 23 cycles. This result suggests that the s-PBI membranes demonstrate excellent in-situ chemical stability in the harsh acid and oxidizing conditions, which agrees well with the ex-situ oxidative stability test results in Table IV that did not detect any degradation after immersion of the s-PBI membranes in the highly oxidative electrolyte for over 400 days.[7] Furthermore, I.V.s of the non-crosslinked s-PBI were measured before and after the long cycling test. The s-PBI gel membrane prepared via PPA process had an initial I.V. of 2.58 dL/g. The I.V. of s-PBI membrane after the long cycling test was 2.25 dL/g and thus appears stable in the sulfuric acid environment.[30]

Conclusions

s-PBI gel membranes were synthesized via the PPA process to afford membranes stable in sulfuric acid and oxidative V(V) solutions. The membranes exhibited high conductivities and good cell performance especially at high current densities. These membranes, however, have inherently high vanadium ion crossover due to the open morphology and low polymer solids content. Vanadium crossover was shown to be inhibited via chemical crosslinks, although still high compared to dense membranes. However, this crosslinking method is transferrable to many PBI chemistries and can be used to further decrease crossover in PBI gel membranes without significant losses in proton conductivity.

Acknowledgments

The information, data, or work presented herein was funded in part by the Advanced Research Projects Agency – Energy (ARPA-E), U. S. Department of Energy, under Award Number DE-AR-0001478.

ORCID

Andrew T. Pingitore https://orcid.org/0000-0002-0860-2909
Zhiwei Yang https://orcid.org/0000-0003-0850-0512
Michael L. Perry https://orcid.org/0000-0003-3313-8498
Brian C. Benicewicz https://orcid.org/0000-0003-4130-1232

References

1. M. L. Perry and A. Z. Weber, *Journal of The Electrochemical Society*, **163**, A5064 (2016).
2. C. Zhang, L. Zhang, Y. Ding, S. Peng, X. Guo, Y. Zhao, G. He, and G. Yu, *Energy Storage Materials*, **15**, 324 (2018).
3. A. Parasuraman, T. M. Lim, C. Menictas, and M. Skyllas-Kazacos, *Electrochimica Acta*, **101**, 27 (2013).
4. W. Xie, R. M. Darling, and M. L. Perry, *Journal of The Electrochemical Society*, **163**, A5084 (2016).
5. C. Fujimoto, S. Kim, R. Stains, X. Wei, L. Li, and Z. G. Yang, *Electrochemistry Communications*, **20**, 48 (2012).
6. S. Chang, J. Ye, W. Zhou, C. Wu, M. Ding, Y. Long, Y. Cheng, and C. Jia, *Surface and Coatings Technology*, **358**, 190 (2019).
7. J. Ye, Y. Cheng, L. Sun, M. Ding, C. Wu, D. Yuan, X. Zhao, C. Xiang, and C. Jia, *Journal of Membrane Science*, **572**, 110 (2019).
8. S. Yun, J. Parrondo, and V. Ramani, *International Journal of Hydrogen Energy*, **41**, 10766 (2016).
9. X. L. Zhou, T. S. Zhao, L. An, L. Wei, and C. Zhang, *Electrochimica Acta*, **153**, 492 (2015).
10. S. Peng, X. Yan, X. Wu, D. Zhang, Y. Luo, L. Su, and G. He, *RSC Advances*, **7**, 1852 (2017).
11. C. Noh, M. Jung, D. Henkensmeier, S. W. Nam, and Y. Kwon, *ACS Appl Mater Interfaces*, **9**, 36799 (2017).
12. K. A. Perry, K. L. More, E. Andrew Payzant, R. A. Meisner, B. G. Sumpter, and B. C. Benicewicz, *Journal of Polymer Science Part B: Polymer Physics*, **52**, 26 (2014).
13. Z. Yuan, Y. Duan, H. Zhang, X. Li, H. Zhang, and I. Vankelecom, *Energy & Environmental Science*, **9**, 441 (2016).
14. T. Luo, O. David, Y. Gendel, and M. Wessling, *Journal of Power Sources*, **312**, 45 (2016).
15. S. Peng, X. Yan, D. Zhang, X. Wu, Y. Luo, and G. He, *RSC Advances*, **6**, 23479 (2016).
16. J.-K. Jang, T.-H. Kim, S. J. Yoon, J. Y. Lee, J.-C. Lee, and Y. T. Hong, *Journal of Materials Chemistry A*, **4**, 14342 (2016).
17. C. Wang, Q. Lai, P. Xu, D. Zheng, X. Li, and H. Zhang, *Adv Mater*, 29 (2017).
18. Y. Zhao, H. Zhang, C. Xiao, L. Qiao, Q. Fu, and X. Li, *Nano Energy*, **48**, 353 (2018).
19. Z. Chang, D. Henkensmeier, and R. Chen, *ChemSusChem*, **10**, 3193 (2017).
20. L. Xiao, H. Zhang, E. Scanlon, L. S. Ramanthan, E. W. Choe, D. Rogers, T. Apple, and B. C. Benicewicz, *Chem. Mater.*, **17**, 5328 (2005).
21. T. R. Garrick, C. H. Wilkins, A. T. Pingitore, J. Mehlhoff, A. Gulledge, B. C. Benicewicz, and J. W. Weidner, *Journal of The Electrochemical Society*, **164**, F1591 (2017).
22. T. R. Garrick, A. Gulledge, J. A. Staser, B. Benicewicz, and J. W. Weidner, *ECS Transactions*, **66**, 31 (2015).
23. W. Li, R. Zaffou, C. Sholvin, M. L. Perry, and Y. She, *ECS Trans.*, **53**, 93 (2013).
24. M. Skyllas-Kazacos, L. Cao, M. Kazacos, N. Kausar, and A. Mousa, *ChemSusChem*, **9**, 1521 (2016).
25. K.-Y. Chan and C. Y. V. Li, *Electrochemically Enabled Sustainability: Devices, Materials and Mechanisms for Energy Conversion*, p. 420, CRC Press (2014).
26. I. B. Valtcheva, P. Marchetti, and A. G. Livingston, *Journal of Membrane Science*, **493**, 568 (2015).
27. Q. Li, J. O. Jensen, R. F. Savinell, and N. J. Bjerrum, *Progress in Polymer Science*, **34**, 449 (2009).
28. M. Razali, C. Didaskalou, J. F. Kim, M. Babaei, E. Drioli, Y. M. Lee, and G. Szekely, *ACS Applied Materials & Interfaces*, **9**, 11279 (2017).
29. J. Yang, H. Jiang, L. Gao, J. Wang, Y. Xu, and R. He, *International Journal of Hydrogen Energy*, **43**, 3299 (2018).
30. J. A. Mader and B. C. Benicewicz, *Macromolecules*, **43**, 6706 (2010).
31. T. Sukkar and M. Skyllas-Kazacos, *Journal of Applied Electrochemistry*, **34**, 137 (2004).
32. Y. Zhang, L. Liu, J. Xi, Z. Wu, and X. Qiu, *Applied Energy*, **204**, 373 (2017).
33. R. M. Darling, A. Smeltz, S. T. Junker, and M. L. Perry, *Distribution of Electrolytes in a Flow Battery*, United States Pat. 9,853,310 (2017).